



Graphene oxide–metallophthalocyanine hybrids with enhanced singlet oxygen generation

Fellipy S. Rocha, Anderson J. Gomes, Claire N. Lunardi*

Laboratory of Photochemistry and Nanobiotechnology, University of Brasilia, Brasilia, DF, Brazil



ARTICLE INFO

Keywords:

Graphene oxide
Zinc phthalocyanine
Singlet oxygen

ABSTRACT

Graphene oxide (GO) was added to zinc phthalocyanine (ZnPc) and tetra nitro substituted zinc phthalocyanine ($\text{ZnPc}(\text{NO}_2)_4$) solutions to evaluate the photophysical interaction of GO with phthalocyanines. Dimethylformamide (DMF) and acetonitrile (MeCN) were used as solvents. GO quenching is shown to be stronger with $\text{ZnPc}(\text{NO}_2)_4$, presenting a Stern-Volmer (K_{sv}) constant approximately 10 times higher than ZnPc. The presence of GO and the increase in its concentration demonstrates a different pattern of absorbance for $\text{ZnPc}(\text{NO}_2)_4$. Singlet oxygen generation was found to be higher in DMF than MeCN enhances with GO present. The overall singlet quantum yield of ZnPc is higher than $\text{ZnPc}(\text{NO}_2)_4$.

1. Introduction

Carbon based nanomaterials exhibit unique mechanical, structural, and electronic properties, and these materials have attracted scientific attention due to the wide applications range [1]. In particular, graphene is a two-dimensional monolayer of sp^2 carbon sheets that are stacked, presenting a honeycomb (hexagonal) crystal lattice, which demonstrates interesting electrical and optical properties [2]. Graphene oxide (GO) is an oxidized form of graphene, containing functional

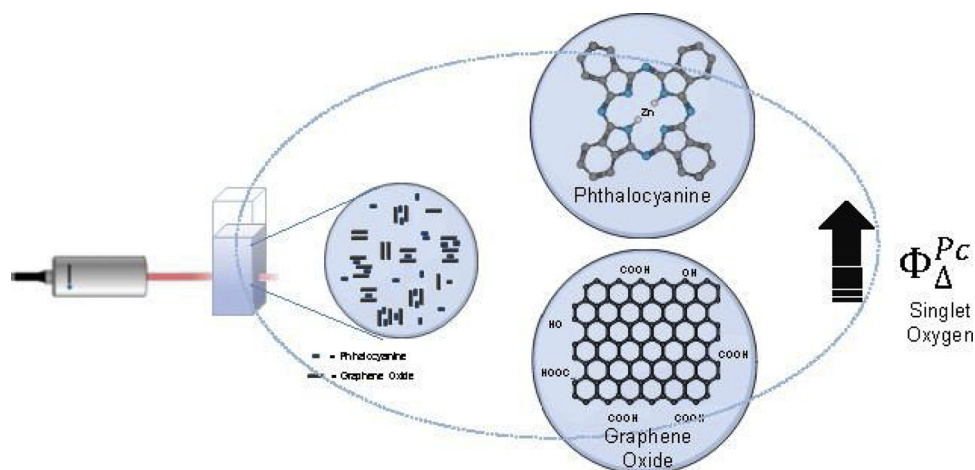
groups exposed over the surface, expanding the capacity to link functional molecules through non-covalent/covalent interaction [3,4]. GO also allows inorganic, organic, and bio-molecules to physically adsorb via strong π - π and electrostatic interactions [5]. Graphene oxide sheets are used to attach biological and chemical drugs, demonstrating potential as a nanocarrier of water-insoluble anticancer drugs. The two-dimensional planar surface of GO confers a high capacity for drug loading, better than other drug-delivery systems [6]. GO is considered relatively biocompatible and is a good candidate for biological applications because it is primarily composed of carbon [7]. However, graphene derivatives generally aggregate in biological or salt solutions, shows a certain degree of cytotoxicity and the loading and release of drugs can be difficult to control [8]. What makes GO more attractive for studies of drug delivery is the presence of functional groups that can be modified by conjugating nanomaterials, enhancing GO stability and biocompatibility [9]. Another approach is based in developing GO nanosheets for in situ simultaneous monitoring of ATP and GTP in

living cells [10], and extraction of polycyclic aromatic hydrocarbons from water samples using GO-polymer composites [11]. Also, sensors [12], solar cells [13], fuel production [14], supercapacitors and energy storage [15] are promising applications of GO-based material. Phthalocyanines are two-dimensional aromatic structures, consisting of four isoindole subunits linked together through nitrogen atoms and present chemical flexibility, making it possible to tailor their physical, optical, and electronic properties. Their electronic delocalization is responsible for numerous features, making them valuable in different fields of science and technology [16,17]. Phthalocyanines have been extensively studied as sensors, low band gap molecular solar cells, nonlinear optical materials, organic field effect transistors, optical information recording media, light-emitting devices, photocatalysts, and photosensitizers for photodynamic therapy (PDT) [18].

Metallophthalocyanines exhibit several characteristic properties, including an intense and broad visible light response (600–800 nm) and high thermal stability [19]. Their photoactivity arises from the extinction of excited triplet oxygen, forming singlet oxygen. Also, conjugation of phthalocyanines with nanoscale materials could enhance their singlet oxygen yield, and this intensified feature is sought to improve the efficiency of PDT treatments [2,20]. Zinc (II) phthalocyanine (ZnPc) complexes have been studied extensively by their photosensitizing properties [21,22]. They present high fluorescent properties, which leads to their extensive use in photodynamic therapy. Moreover, the particular chemical groups at the periphery of zinc phthalocyanine compounds may be selectively preferred by some tumor cells, and phthalocyanines with these structures are called third

* Corresponding author.

E-mail addresses: fellipysr@gmail.com (F.S. Rocha), ajgomes@unb.br (A.J. Gomes), clunardi@unb.br (C.N. Lunardi).



Scheme 1. Metallophthalocyanine and graphene oxide interaction in organic solvent.

generation photosensitizers [23]. Tetra substituted phthalocyanines may be preferred when their functionality and solubility are taken into consideration because they offer higher stability as well. Functional phthalocyanines are more favored than other forms due to their advanced features.

Studies regarding the interactions between GO and phthalocyanines (Pc) in several medium are sparse, and understanding this process is a crucial step to support the GO–Pc hybrid material as a potential photosensitizer for PDT applications. Moreover, nature, specificity, and mechanisms driving the GO–Pc interactions need to be elucidated. In this study, we aimed to investigate several aspects of GO–Pc hybrid formation (aggregation behavior, fluorescence quenching, binding kinetics, and oxygen singlet generation). Here, we provide a comprehensive study of GO interaction with zinc phthalocyanine and tetra-nitro substituted zinc phthalocyanine in organic solvents (Scheme 1).

2. Material and methods

GO (1 mg/mL), ZnPc (powder), and DPBF (powder) were obtained commercially from Sigma- Aldrich. Before utilization, GO and ZnPc solutions were submitted to sonication for 5–10 min.

ZnPc(NO₂)₄ was synthesized through the tetramerization of 4-nitrophthalonitrile in the presence of 1,8-diazabicyclo [5,4,0]undec-7-ene (DBU) and zinc acetate, as reported by Lunardi [24].

2.1. Preparation of the GO–Pc hybrids

Phthalocyanine solutions (ZnPc and ZnPc(NO₂)₄) were fixed at 10 μM and mixed with increasing concentrations of the GO solution (0–12 μg/mL), then sonicated for 5–10 min before characterization.

2.2. Steady state spectral measurement

The absorption and emission spectra were recorded on a Hitachi UV–vis U-900H spectrophotometer and a spectrophotometer of fluorescence from Hitachi High-Technologies Corporation®, model F-7000, respectively. All spectra were recorded with appropriate background corrections. The concentrations of GO used in the different experiments have been specified in the context. The experiments were carried out at room temperature (300 K).

2.3. Fluorescence quenching analysis

For ideal cases of quenching, the following well-known Stern-Volmer equation was applied:

$$\frac{I_F^0}{I_F} = 1 + Kq\tau_0[Q] = 1 + K_{sv}[Q] \quad (1)$$

where I_F^0 is the fluorescence intensity, I_F is the equivalent parameter in the presence of the quencher (GO) at a concentration $[Q]$, k_q is the quenching rate constant of the bio-molecule, I_F^0 is the average lifetime of the fluorescent substance without any quencher, and I_F^0 is the Stern-Volmer quenching constant. Hence, Eq. (1) can be used to determine by linear regression of a plot of $\frac{I_F^0}{I_F}$ against $[Q]$ and $Kq = \frac{K_{sv}}{\tau_0}$ [25]. The parameters of the association of ZnPc and ZnPc(NO₂)₄

with GO were derived based on the Hill equation, as follows:

$$Q = \frac{(I^0 - I)}{I^0} \quad (2)$$

$$\frac{Q}{Q_{\max}} = \frac{[GO]^n}{(K_D^n + [GO]^n)} \quad (3)$$

where Q_{\max} is the saturation value of Q , KD , is the equilibrium binding dissociation constant, which describes the relative strength of the GO–fluorophore interaction, and n represents the Hill coefficient, which defines the cooperativity association [26].

2.4. Singlet oxygen quantum yield measurements

Singlet oxygen quantum yield ($\Phi\Delta$) is typically carried out using the chemical trapping method [27]. For assays, 30 μL of DPBF were added to 2.5 mL of 5 μM solutions with ZnPc or ZnPc(NO₂)₄ and were irradiated at 637 nm using a laser with 25 mW. Experiments were performed under air conditions and at ambient temperature. The kinetic constant of DPBF photodegradation (K_{DPBF}) was determined by applying the first order kinetic model equation, as follows:

$$kt = Ln \frac{(A_0 - A_{inf})}{(A - A_{inf})} \quad (4)$$

where A_0 and A_{inf} are the DPBF absorbances at zero and infinite time, respectively. The singlet oxygen quantum yield ($\Phi\Delta$) was determined by the following equation:

$$\frac{\Phi_{Pc}}{\Delta} = \frac{\Phi_{Std}}{\Delta} \frac{r_{DPBF}^{Pc} (1 - 10(A_{637Std}))}{r_{DPBF}^{Std} (1 - 10(A_{637Pc}))} \quad (5)$$

where $\Phi\Delta$ represents the singlet oxygen quantum yield ($\Phi\Delta = 0.5639$ for the standard ZnPc in DMF), r_{DPBF}^{Pc} and r_{DPBF}^{Std} represent the DPBF photobleaching rates (kinetic constants, k and k_{std} , respectively), $(1-10A_{637Std})$ and $(1-10A_{637Pc})$ represent the fraction of absorbed light at the irradiation wavelength, and A_{637Std} and A_{637Pc} represent the absorbance at the irradiation wavelength of the standard ZnPc (Std) and other phthalocyanines (Pc), respectively [28].

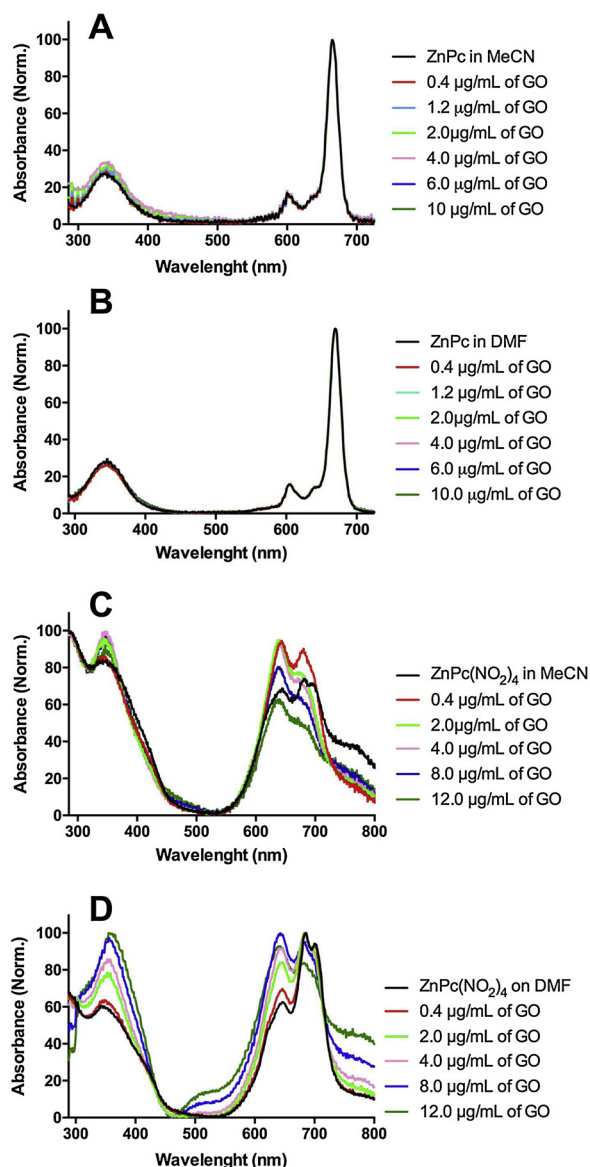


Fig. 1. Normalized absorption spectrum of ZnPc in (A) MeCN and (B) DMF and ZnPc(NO₂)₄ in (C) MeCN and (D) DMF.

3. Results and discussion

ZnPc was obtained commercially from Sigma-Aldrich and ZnPc(NO₂)₄ was synthesized using a well-known route [24]. Characterization of the interaction of ZnPc and ZnPc(NO₂)₄ with GO was performed using two organic solvents, dimethylformamide (DMF) and acetonitrile (MeCN). We aimed to investigate the photophysical characteristics of the phthalocyanines interaction with GO, employing spectroscopic techniques, such as ultraviolet-visible (UV-vis) for aggregation, singlet oxygen evaluations and fluorescence emission for quenching and binding kinetics. The UV-vis absorption spectroscopic technique can characterize the intermolecular association of monomers [29]. The amount of GO plays a critical role in the aggregation process; thus, the determination of its optimal concentration is necessary [30]. We present the absorbance intensity of the phthalocyanines (10 µM) with an increasing GO ratio (Fig. 1).

The ground state electronic absorption spectra of phthalocyanine compounds show two dominant absorption bands in the ultraviolet and visible region. These absorption bands are known as B (Soret) and Q bands, respectively. The Q band is observed at around 600–750 nm

due to the π - π transitions from the highest occupied molecular orbital (HOMO) to the lowest unoccupied molecular orbital (LUMO) of the Pc ring. The B band is observed at around 300–450 nm, arising from deeper π levels to the LUMO transition [31]. The non-substituted Pc (ZnPc) shows (Fig. 1A and B) a typical electronic absorption spectrum of a metallated Pc complex with monomeric behavior, evidenced by a single (narrow) Q band at 665 nm for acetonitrile (Fig. 1A) and at 670 nm DMF (Fig. 1B). The presence of GO does not stimulate the formation of dimers and aggregates due to no observed widening or split of the Q band, which preserved the ZnPc monomeric behavior, and the absorption intensity remained unaltered. Similar behavior was described for phthalocyanines interaction with graphene quantum dots in organic solvents [32].

On the other hand, tetra nitro substituted Pc (ZnPc(NO₂)₄) shows (Fig. 1C and D) a more broader Q band, with a Q_x Q_y split, characterizing non-monomeric behavior, which was already expected since the solution of ZnPc(NO₂)₄ was a mixture of structural isomers. The Pc presents a Q_x band at 640 nm and a higher intensity Q_y band at 680 nm in MeCN (Fig. 1C). In DMF (Fig. 1D), ZnPc(NO₂)₄ exhibits a Q_x band at 647 nm and a stronger Q_y band at 685 nm with a shoulder at 700 nm. Initially, with GO addition in the MeCN solution the absorption intensity increases for the whole Q band with the Q_x band presenting the highest magnitude, while in DMF only the Q_x band increases and do not surpass the Q_y band absorption. After increasing the GO concentration in MeCN, the phthalocyanine Q_x band weakens while the blue-shifted Q_y band tended to fade. In the DMF solution, the Q_x band also blue-shifts and decreases. Thus, these changes in the absorption spectrum of ZnPc(NO₂)₄ could be explained by the π - π stack of tetra nitro substituted Pc isomers with GO.

Fluorescence quenching can serve as a valuable source of information regarding biochemical systems. A significant number of recent studies on fluorescence quenching of organic dyes by graphene have emerged, while similar reports linked to GO remain sparse [33]. Fluorescence quenching measurements can reveal the accessibility of Pc to GO groups, helping explain ligand-binding mechanisms, providing clues to the nature of the binding phenomenon. It can also be used to discover unique structural and dynamic information. The formation of H-aggregates (face-to-face arrangement of the monomer) is characterized by a blue-shift in the UV-vis spectra and a well-documented fluorescence quenching, where the electron transition to the HOMO is allowed and is followed by a rapid conversion of this excited state to the LUMO, quenching the fluorescence as a result [34].

Fluorescence quenching is a process that decreases the fluorescence intensity of a fluorophore. It is known that non-covalent attachment of fluorophores to the GO surface results in fluorescence quenching, which is induced by two simultaneous processes, energy transfer (ET) and photo-induced electron transfer (PET), from the electron donor metallophthalocyanines to the electron acceptor GO [35]. The fluorescence emission peak of ZnPc(NO₂)₄ (Fig. 2E and F) is remarkably extinct under the presence of GO and nearly vanishes when GO concentration is increased, demonstrating immediate and strong adsorption onto the GO surface. In some studies, the strong π - π stacking effect and electrostatic interaction between GO and fluorophores is attributed to the high quenching efficiency of GO [36]. The effect of GO is similarly observed for other dyes, and its role in the quenching process has been discussed in detail [37,38]. Bagio et al. demonstrates that for aqueous soluble phthalocyanine like AlClPc, its association to graphene oxide quenches fluorescence emission and suppresses ROS generation. This effect is attributed to electron donor-acceptor interactions and the coordination of oxygenated groups in graphene oxides with the central Al cation of phthalocyanine [39]. Similar behavior was also reported for CoPc-GO nanocomposites [40].

However, in this study ZnPc, fluorescence intensity (Fig. 2E and F) shows little changes under the presence of GO in organic medium. The unexpected weak quenching effect for unsubstituted zinc phthalocyanine could be related to a slight rotational twist in the interaction

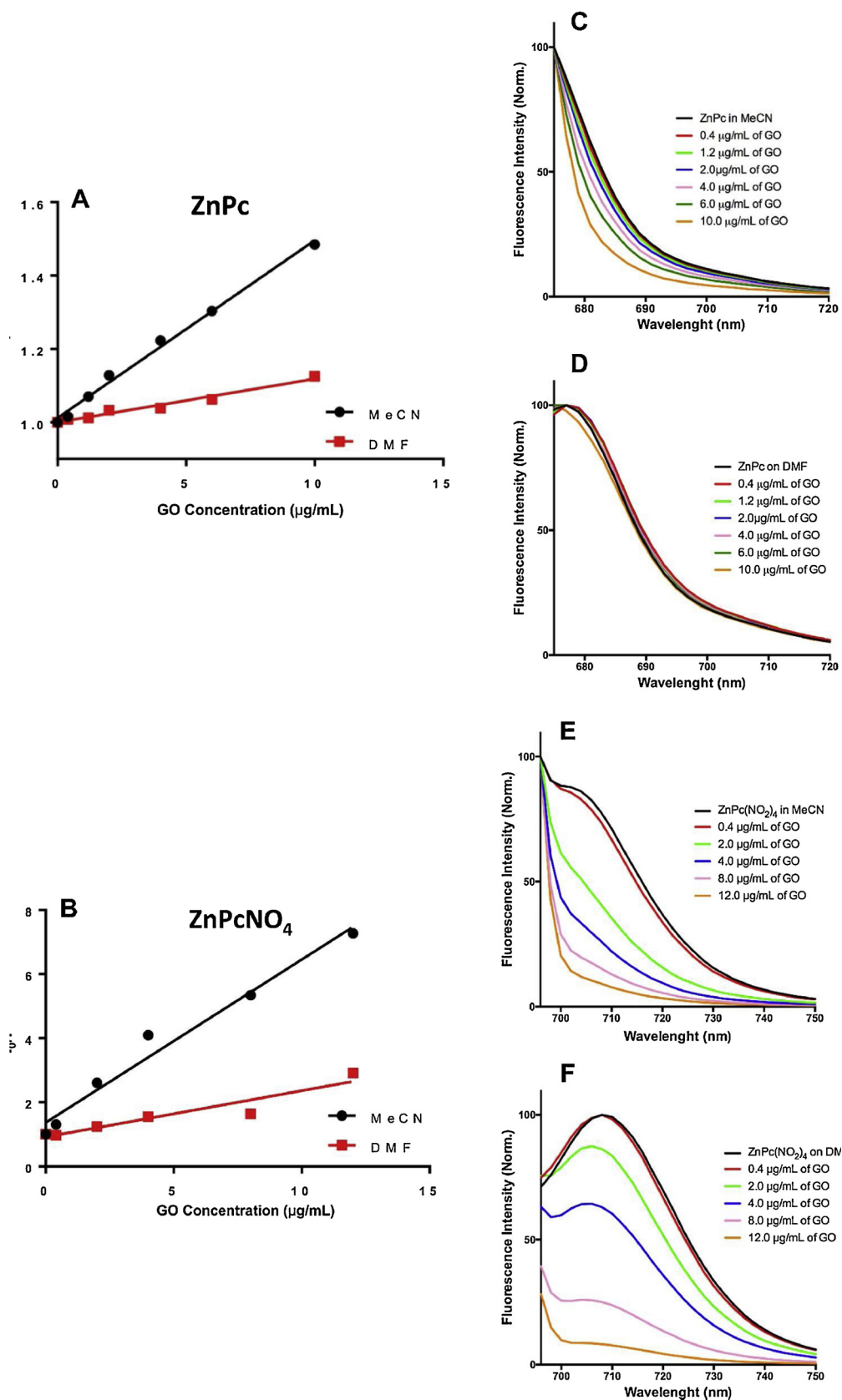


Fig. 2. Stern-Volmer plot of the fluorescence quenching efficiency of (A) ZnPc ($\lambda_{ex} = 670$ nm) and (B) ZnPc(NO₂)₄ ($\lambda_{ex} = 685$ nm). The inset figures show the fluorescence quenching efficiency.

angle, disorienting the π - π stacking process [41].

We also noted shifts in the fluorescence emission maximum wavelength λ_{\max} of ZnPc(NO₂)₄, although no shifts were observed for ZnPc. The inset of Fig. 2F shows that the GO presence in the DMF solution induces a blue-shift of λ_{\max} from 708 nm to ~705 nm. For the MeCN solution (Fig. 2E), it is hard to determine if there was any shift because of the peak format and a substantial depletion of fluorescence emission. Relevant information may be revealed by a change of the λ_{\max} regarding the microenvironment of the GO–ZnPc(NO₂)₄ interaction. For biological molecules, a blue-shift usually indicates that the fluorescent agent is exposed to a more hydrophobic environment, and a red-shift implies an increase in polarity and hydrophilicity of the local molecular environment [25,26]. In theory, loading of the tetra substituted phthalocyanine onto the GO surface by π - π stacking should enhance the hydrophobicity of the environment of the fluorophore, and the presented blue-shift is a good indication of a successful load.

Stern-Volmer (SV) equation was applied to analyze fluorescence emission data [42], assuming

that the interaction of phthalocyanine with GO occurs under equilibrium conditions. To explain the fluorescence quenching process, two mechanisms are shown to exist mainly as dynamic and static quenching, and this process can be due to the transfer of electrons in the excited state from the dye to GO, which acts like an electron acceptor [38]. Dynamic quenching occurs when the lifetime of the excited fluorophore decreases, and for static quenching the lifetime remains the same [43]. It is known that fluorescence quenching is primarily driven by diffusive transport at low nanomaterial concentrations [44]. A linear pattern is observed in the SV plot (Fig. 2A and B), and there is substantial evidence that the fluorescence quenching process is mainly driven by a dynamic (collisional) effect, which occurs due to weak coupling of ZnPc and ZnPc(NO₂)₄ at the GO surface. ZnPc expresses K_{sv} values of $(1.18 \pm 0.08) \times 10^{-2} \text{ M}^{-1}$ in DMF and $(4.84 \pm 0.17) \times 10^{-2} \text{ M}^{-1}$ in MeCN, and ZnPc(NO₂)₄ expresses K_{sv} values of $(14.43 \pm 2.5) \times 10^{-2} \text{ M}^{-1}$ in DMF and $(50.86 \pm 4.19) \times 10^{-2} \text{ M}^{-1}$ in MeCN. These values show that the K_{sv} value of the tetra-substituted phthalocyanine is 10 times higher in both solvents than the non-substituted Pc, and the K_{sv} value is about 4 times higher in MeCN than in DMF solution for both dyes.

To evaluate the strength and cooperativity of the GO–ZnPc and GO–ZnPc(NO₂)₄ interaction, we applied the mathematical model of Hill because the amount of template material plays a critical role in the molecular aggregation process. The GO sheets lead to a perfect interaction orientation as H aggregates under optimal conditions due to the π - π and electrostatic cooperative interactions of the dye and GO [29]. Thus, it is necessary to quantify key parameters describing the association between phthalocyanines and GO, i.e., the saturation value Q , binding dissociation constant K_D , and the Hill coefficient n , assuming that the binding of phthalocyanine to GO occurs under equilibrium conditions [26].

The interaction of the tetra substituted dye with GO (Fig. 3) shows a higher Q value than the

non-substituted dye, and for both phthalocyanines there is a higher saturation value using MeCN as the solvent. ZnPc and GO interactions in DMF suggest a sigmoidal curve, indicating that there is more than one binding site that exhibits positive or negative cooperativity [45]. The interaction of GO with ZnPc in MeCN and ZnPc(NO₂)₄ in both solvents presented a Hill coefficient around 1, and for ZnPc in DMF the Hill coefficient was 5.34. When n is around 1 this indicates an independent binding process, and the interaction is probably happening under optimal conditions, leading to the formation of H-type aggregates, which corroborate with the blue-shift observed in the ZnPc(NO₂)₄ UV-vis spectra. For n values significantly different from 1.0 this implies that the interaction is more complex, and a simple second order reaction is inadequate description of the reaction and a more detailed kinetic analysis may be required [46]. As ZnPc presented a weak quenching effect and the sigmoidal Hill plot and n were significantly

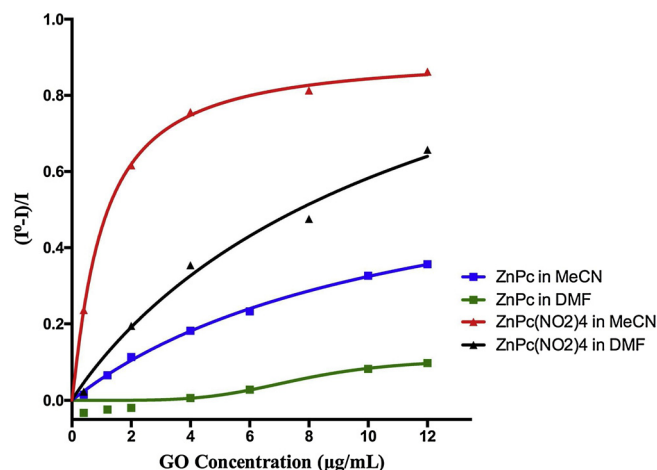


Fig. 3. Hill plot of the fluorescence quenching of ZnPc and ZnPc(NO₂)₄ in the presence of GO with increasing concentrations.

different from 1, we suggest that the binding with GO exhibits negative cooperativity due to the interaction angle rotational twist, and the description of the interaction between monomer transition dipoles in molecular dimers can help elucidate if a more complicated vibrational structure is taking place [47]. The solution of ZnPc(NO₂)₄ in MeCN exhibits the lowest K_d value of $1.015 \pm 0.182 \mu\text{M}$, while ZnPc shows the highest K_d value of $11.000 \pm 1.613 \mu\text{M}$ in the same solvent. ZnPc(NO₂)₄ and ZnPc in DMF solution presents similar K_d values of $6.692 \pm 2.044 \mu\text{M}$ and $7.050 \pm 1.712 \mu\text{M}$ respectively. However, there is no systematic data available in the literature regarding the number of binding sites and the association constants for GO interaction with phthalocyanines. A similar system with tetrasulfonated phthalocyanines binding to prion proteins presents a K_d value of $8.5 \mu\text{M}$ [48] and another system with sulfonated aluminum phthalocyanine binding in human serum albumin presents a K_d value of $2.5 \mu\text{M}$ [49].

Singlet oxygen is generated when an activated sensitizer in its excited triplet state interacts with oxygen in its ground triplet state. Evaluation of the ability of novel phthalocyanines to produce reactive oxygen species in organic solvents and aqueous solutions can be valuable for predicting in vitro activity against cancerous cells or microorganisms [50]. The photodynamic activities of free ZnPc and ZnPc(NO₂)₄ were evaluated and compared against GO–ZnPc and GO–ZnPc(NO₂)₄ hybrids. The ability of the phthalocyanines to produce singlet oxygen ($^1\text{O}_2$) was tracked using 1,3-diphenylisobenzofuran (DPBF), verifying the decrease in DPBF absorbance, monitored at 417 nm during irradiation with a red laser, as shown in Fig. 4. The DPBF indirect method has been widely used to provide a quantitative analysis of singlet oxygen production since the reaction product (1,2-dibenzylbenzene) does not absorb visible light. This technique correlates the reduction of DPBF absorbance and the amount of oxygen quantum yield generated by a type II photo process [51].

ZnPc and ZnPc(NO₂)₄ photobleaching was not verified since the Q absorption band at 670 nm and 685 nm, respectively, remains unchanged. DPBF photodegradation can be visually monitored by the color change of the solution from yellow to colorless when irradiated by a 637 nm red laser (25 mW). The photodegradation of DPBF by free phthalocyanines and GO–ZnPc and GO–ZnPc(NO₂)₄ followed typical first order kinetics, as illustrated in the insets of Fig. 4.

The singlet oxygen quantum yield (Φ_Δ) is the most critical parameter to evaluate in photodynamic activity. The Φ_Δ is the ratio of the number of produced $^1\text{O}_2$ molecules to the number of photons absorbed by the photosensitizer [52]. A precise determination of Φ_Δ is difficult due to the aggregation of the photosensitizer in solution, which reduces its photobiological activity. Aggregation is associated with a red-shift (bathochromic displacement) or a blue-shift (hypochromic

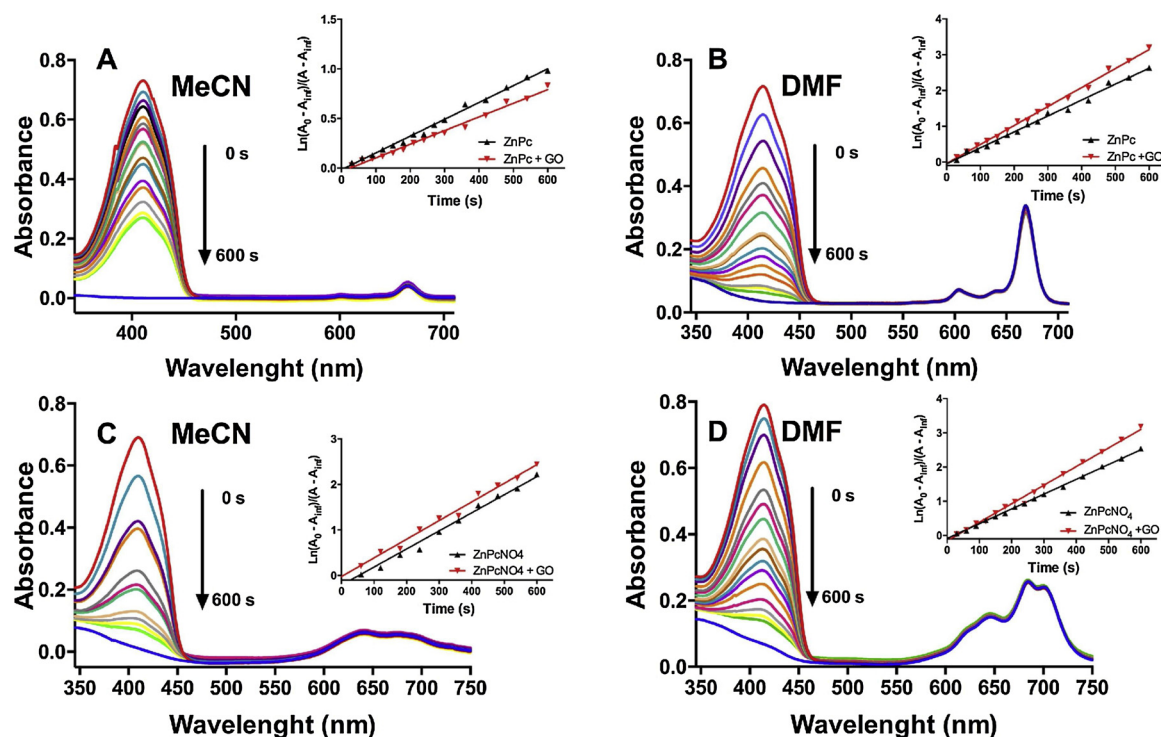


Fig. 4. Photodegradation of DPBF by red laser irradiation in the presence of ZnPc and ZnPc(NO₂)₄ associated with GO in MeCN and DMF. The photodegradation followed the same pattern of absorbance decrease for the free phthalocyanines. The inset figures show first order kinetics. (A) ZnPc in MeCN, (B) ZnPc in DMF, (C) ZnPc(NO₂)₄ in MeCN, and (D) ZnPc(NO₂)₄ in DMF (For interpretation of the references to colour in this figure legend, the reader is referred to the web version of this article).

displacement) of the Q band, and no shifts were observed during the photobleaching tests [53].

In general, substituted derivatives show lower singlet oxygen quantum yields [54]. As can be observed in Table 1, the overall values of Φ_{Δ} for ZnPc are higher than for ZnPc(NO₂)₄, as expected. The singlet quantum yield of ZnPc was higher than ZnPc(NO₂)₄ high production of the excited triplet state, results in reasonably high singlet oxygen quantum yields, though competing processes like phosphorescence and non-radiative decay may lower the yield for singlet oxygen production. The literature [11] shows that unsubstituted ZnPc has a relatively high triplet lifetime of 300 μ s and a higher singlet oxygen quantum yield as compared to the other complexes. However, the ZnPc(NO₂)₄ compound has a high HOMO (Highest Occupied Molecular Orbital) energy level. The 1O₂ production of the compounds with high HOMO energy level can be effectively reduced by polar solvents.

When the dyes interact with GO, Φ_{Δ} increase, displaying excellent ability to generate singlet oxygen with relatively high potential to be employed in PDT, and this effect has already been observed for methylene blue [55]. The fluorescence enhancement of tetrasulfonated zinc phthalocyanine by graphene derivatives has already been reported [56], suggesting that graphene quantum dots (GQDs) enhance

the fluorescence quantum yield of one abnormal fluorescence peak from the phthalocyanine triplet excited state. Other GQDs interaction with ZnTPPCQ showed an increase of singlet oxygen quantum yield suggested by the increase in π bonds [32]. High triplet quantum yield with a corresponding low fluorescence quantum yield suggests a more efficient intersystem crossing, which is desirable for a compound that may be used as a photosensitizer. The ability of a molecule to be long-lived and to populate the triplet state is essential since this has a direct bearing on singlet oxygen production [57]. Another feature is the solvent effect in the singlet oxygen generation, higher in DMF than MeCN. As described solvent effects on photosensitizing ability could be due to relative shifts in the positions of the photosensitizer's singlet and triplet excited states. In some solvents, the separation between the singlet and triplet may be maximal, resulting in a low intersystem crossing rate [58,59]. With increasing solvent polarity, the energy gap between

the triplet state and the singlet state increases, and thereby reduces intersystem crossing (MeCN is more polar than DMF). This, in turn, reduces the yield of singlet oxygen produced by energy transfer from the triplet state of the GO-phthalocyanine hybrid.

4. Conclusions

In summary, we prepared and characterized two Go-Pc photoactive hybrid materials by a simple method. The GO-ZnPc(NO₂)₄ hybrid presented an immediate and strong π - π stacking interaction, confirmed by absorption and fluorescence spectra, while no evidence of strong π - π stacking was observed for the GO-ZnPc hybrid. The Stern-Volmer mathematical method suggests that the interaction of GO is 10 times stronger with ZnPc(NO₂)₄ compared to ZnPc, and its linear slope graph plot showed that the interaction is mainly driven by a collisional effect. The Hill coefficient calculated indicates an independent binding process for GO-ZnPc(NO₂)₄ hybrid formation, leading to the formation of H-type aggregates by strong π - π stacking and a more tricky binding

Table 1

DPBF photobleaching rate constants (kDPBF) and singlet oxygen quantum yields (Φ_{Δ}) for free ZnPc and ZnPc(NO₂)₄, GO-ZnPc, and GO-ZnPc(NO₂)₄.

Free Phthalocyanines	kDPBF(s ⁻¹)	Φ_{Δ}
ZnPc DMF	$(4.45 \pm 0.20) \times 10^{-3}$	0.5639
GO-ZnPc DMF	$(5.31 \pm 0.18) \times 10^{-3}$	0.71 ± 0.008
ZnPc MeCN	$(1.69 \pm 0.001) \times 10^{-3}$	0.50 ± 0.002
GO-ZnPc MeCN	$(1.37 \pm 0.001) \times 10^{-3}$	0.71 ± 0.012
ZnPc(NO ₂) ₄ DMF	$(4.32 \pm 0.10) \times 10^{-3}$	0.25 ± 0.005
GO-ZnPc(NO ₂) ₄ DMF	$(5.43 \pm 0.24) \times 10^{-3}$	0.32 ± 0.001
ZnPc(NO ₂) ₄ MeCN	$(3.97 \pm 0.38) \times 10^{-3}$	0.27 ± 0.014
GO-ZnPc(NO ₂) ₄ MeCN	$(4.09 \pm 0.29) \times 10^{-3}$	0.29 ± 0.007

process for the GO–ZnPc hybrid. The phthalocyanines presents a higher singlet oxygen quantum yield associated with GO and remained stable during all tests. Future research on decay lifetimes might extend the explanations of GO–Pc interaction mechanisms in different solvents. Overall, our results demonstrate a strong effect of solvent and type of substitution on metallophthalocyanines in the preparation and properties of formed hybrids. In conclusion, it would appear that the prepared hybrids are promising photosensitizer candidates for PDT, specially GO–ZnPc(NO₂)₄.

Acknowledgements

The authors acknowledge the financial support from the University of Brasília, the Coordination for the Improvement of Higher Educational Personnel (CAPES code 001), the Federal District Research Foundation (FAPDF), the Scientific and Technological Development Foundation (FINATEC), and the National Council for Scientific and Technological Development (CNPq) to conceive this work. F.S.R., A.J.G, and C.N.L.G. conceived and designed the research. F.S.R carried out the experiments. F.S.R and C.N.L.G. interpreted the results and wrote the manuscript. The authors declare no competing financial interests.

References

- Z. Wang, C. He, W. Song, Y. Gao, Z. Chen, Y. Dong, C. Zhao, Z. Li, Y. Wu, *RSC Adv.* 5 (2015) 94144–94154.
- Y. Wan, Q. Liang, T. Cong, X. Wang, Y. Tao, M. Sun, Z. Li, S. Xu, *RSC Adv.* 5 (2015) 66286–66293.
- X. Sun, Z. Liu, K. Welscher, J.T. Robinson, A. Goodwin, S. Zaric, H. Dai, *Nano Res.* 1 (2008) 203–212.
- T. Kuila, S. Bose, A.K. Mishra, P. Khanra, N.H. Kim, J.H. Lee, *Prog. Mater. Sci.* 57 (2012) 1061–1105.
- E. Bozkurt, M. Acar, Y. Onganer, K. Meral, *Phys. Chem. Chem. Phys.* 16 (2014) 18276–18281.
- G. Shim, M.-G. Kim, J.Y. Park, Y.-K. Oh, *Adv. Drug Deliv. Rev.* 105 (2016) 205–227.
- Z. Zhu, J. Qian, X. Zhao, W. Qin, R. Hu, H. Zhang, D. Li, Z. Xu, B.Z. Tang, S. He, *ACS Nano* 10 (2015) 588–597.
- Z. Wang, L.C. Ciacchi, G. Wei, *Appl. Sci.* 7 (2017) 1175.
- C. McCallion, J. Burthem, K. Rees-Unwin, A. Golovanov, A. Pluen, *Eur. J. Pharm. Biopharm.* 104 (2016) 235–250.
- Y. Wang, L. Tang, Z. Li, Y. Lin, J. Li, *Nat. Protoc.* 9 (2014) 1944.
- Y.-B. Luo, J.-S. Cheng, Q. Ma, Y.-Q. Feng, J.-H. Li, *Anal. Methods* 3 (2011) 92–98.
- D. Chen, H. Feng, J. Li, *Chem. Rev.* 112 (2012) 6027–6053.
- H. Zhang, W. Wang, H. Liu, R. Wang, Y. Chen, Z. Wang, *Mater. Res. Bull.* 49 (2014) 126–131.
- W. Xie, M. Huang, *Energy Convers. Manage.* 159 (2018) 42–53.
- K.Y. Kumar, S. Archana, R. Namitha, B.P. Prasanna, S.C. Sharma, M.S. Raghu, *Mater. Res. Bull.* 107 (2018) 347–354.
- C.N. Lunardi, A.C. Tedesco, *Curr. Org. Chem.* 9 (2005) 813–821.
- C.G. Claessens, U. Hahn, T. Torres, *Chem. Rec.* 8 (2008) 75–97.
- E. Gürel, M. Pişkin, S. Altun, Z. Odabas, M. Durmus, *Dalton Trans.* 44 (2015) 6202–6211.
- S.F. Pop, R.M. Ion, *J. Optoelectron. Adv. Mater.* 12 (2010) 1976–1980.
- M.E. Wieder, D.C. Hone, M.J. Cook, M.M. Handsley, J. Gavrilovic, D.A. Russell, *Photochem. Photo-biol. Sci.* 5 (2006) 727–734.
- P.C. Martin, M. Gouterman, B.V. Pepich, G.E. Renzoni, D.C. Schindele, *Inorg. Chem.* 30 (1991) 3305–3309.
- K. Tabata, K. Fukushima, K. Oda, I. Okura, *J. Porphy. Phthalocyanines* 4 (2000) 278–284.
- A. Ogunsipe, D. Maree, T. Nyokong, *J. Mol. Struct.* 650 (2003) 131–140.
- C.N. Lunardi, J.C. Rotta, A.C. Tedesco, *J. Porphy. Phthalocyanines* 7 (2003) 493–499.
- M.A. Rashid, S.N.I. Rabbi, T. Sultana, M.Z. Sultan, M.Z. Sultan, *Pharm. Anal. Acta* 6 (2015) 408.
- K.P. Loh, C.T. Lim, et al., *Nanoscale* 8 (2016) 9425–9441.
- X.-F. Zhang, Y. Lin, W. Guo, J. Zhu, *Spectrochim. Acta Part A: Mol. Biomol. Spectrosc.* 133 (2014) 752–758.
- F. Li, Q. Liu, Z. Liang, J. Wang, M. Pang, W. Huang, W. Wu, Z. Hong, *Org. Biomol. Chem.* 14 (2016) 3409–3422.
- C. Hansda, U. Chakraborty, S.A. Hussain, D. Bhattacharjee, P.K. Paul, *Spectrochim. Acta Part A: Mol. Biomol. Spectrosc.* 157 (2016) 79–87.
- M. g'lu, B. Gür, M. Ar, Y. Onganer, K. Meral, *RSC Adv.* 3 (2013) 11832–11838.
- M. Göksel, M. Durmus, D. Atilla, *Photochem. Photobiol. Sci.* 15 (2016) 1318–1329.
- R. Matshitse, T. Nyokong, *J. Fluoresc.* 28 (2018) 827–838.
- K. li Fan, Z. kun Guo, Z. gang Geng, J. Ge, S. long Jiang, J. hua Hu, Q. Zhang, *Chin. J. Chem. Phys.* 26 (2013) 252–258.
- N. Kundu, A. Roy, D. Banik, J. Kuchlyan, N. Sarkar, *J. Phys. Chem. C* 119 (2015) 25023–25035.
- Z. Li, C. He, Z. Wang, Y. Gao, Y. Dong, C. Zhao, Z. Chen, Y. Wu, W. Song, *Photochem. Photobiol. Sci.* 15 (2016) 910–919.
- X. Qi, K.-Y. Pu, X. Zhou, H. Li, B. Liu, F. Boey, W. Huang, H. Zhang, *Small* 6 (2010) 663–669.
- Y. Liu, C. yan Liu, Y. Liu, *Appl. Surf. Sci.* 257 (2011) 5513–5518.
- T. Tachikawa, S.-C. Cui, M. Fujitsuka, T. Majima, *Phys. Chem. Chem. Phys.* 14 (2012) 4244–4249.
- A.R. Baggio, M.S. Santos, F.H. Souza, R.B. Nunes, P.E.N. Souza, S.N. Bão, A.O.T. Patrocínio, D.W. Bahnemann, L.P. Silva, M.J.A. Sales, et al., *J. Phys. Chem. A* 122 (2018) 6842–6851.
- J.-H. Yang, Y. Gao, W. Zhang, P. Tang, J. Tan, A.-H. Lu, D. Ma, *J. Phys. Chem. C* 117 (2013) 3785–3788.
- U. Rösch, S. Yao, R. Wortmann, F. Würthner, *Angew. Chem.* 118 (2006) 7184–7188.
- H. Zeng, G. Durocher, *J. Lumin.* 63 (1995) 75–84.
- S. Doose, H. Neuweiler, M. Sauer, *ChemPhysChem* 10 (2009) 1389–1398.
- S.H.D.P. Lacerda, J.J. Park, C. Meuse, D. Pristinski, M.L. Becker, A. Karim, J.F. Douglas, *ACS Nano* 4 (2009) 365–379.
- T.-C. Chou, P. Talalay, *Adv. Enzyme Regul.* 22 (1984) 27–55.
- G.A. Weiland, P.B. Molinoff, *Life Sci.* 29 (1981) 313–330.
- S. Yanagisawa, T. Yasuda, K. Inagaki, Y. Morikawa, K. Manseki, S. Yanagida, *J. Phys. Chem. A* 117 (2013) 11246–11253.
- D.R. Dee, A.N. Gupta, M. Anikovskiy, I. Sosova, E. Grandi, L. Rivera, A. Vincent, A.M. Brigley, N.O. Petersen, M.T. Woodside, *Biochim. Biophys. Acta (BBA)-Proteom. Proteom.* 1824 (2012) 826–832.
- T.G. Gantchev, R. Ouellet, J.E. van Lier, *Arch. Biochem. Biophys.* 366 (1999) 21–30.
- J. Długaszewska, W. Szczolko, T. Koczorowski, P. Skupin-Mrugalska, A. Teubert, K. Konopka, M. Kucinska, M. Murias, N. Düzgünes, J. Mielcarek, et al., *J. Inorg. Biochem.* 172 (2017) 67–79.
- X.-F. Zhang, X. Li, *J. Lumin.* 131 (2011) 2263–2266.
- M.P. Romero, N.R. Gobo, K.T. de Oliveira, Y. Iamamoto, O.A. Serra, S.R. Louro, *J. Photochem. Photobiol. A: Chem.* 253 (2013) 22–29.
- T.D. de Souza, F.I. Ziembowicz, D.F. Müller, S.C. Laueremann, C.L. Kloster, R.C.V. Santos, L.Q.S. Lopes, A.F. Ourique, G. Machado, M.A. Villetti, *Eur. J. Pharm. Sci.* 83 (2016) 88–98.
- M. Kucinska, P. Skupin-Mrugalska, W. Szczolko, L. Sobotta, M. Sciepora, E. Tykarska, M. Wierzchowski, A. Teubert, A. Fedoruk-Wyszomirska, E. Wyszko, et al., *J. Med. Chem.* 58 (2015) 2240–2255.
- M. Wojtoniszak, D. Rogin'ska, B. Machalin'ski, M. Drozdziak, E. Mijowska, *Mater. Res. Bull.* 48 (2013) 2636–2639.
- G. Fomo, O.J. Achadu, T. Nyokong, *J. Mater. Sci.* 53 (2018) 538–548.
- N. Nwihara, J. Britton, T. Nyokong, *J. Coord. Chem.* 70 (2017) 1601–1616.
- A. Ogunsipe, J.-Y. Chen, T. Nyokong, *New J. Chem.* 28 (2004) 822–827.
- S.K. Lower, M.A. El-Sayed, *Chem. Rev.* 66 (1966) 199–241.